ISSN 0001-4370, Oceanology, 2023, Vol. 63, No. 2, pp. 149–156. © Pleiades Publishing, Inc., 2023.
Russian Text © The Author(s), 2023, published in Okeanologiya, 2023, Vol. 63, No. 2, pp. 173–181.

MARINE PHYSICS

# Impact of the Atlantic Meridional Overturning Circulation on the Upper Water Temperature of the North Atlantic and the Atlantic Sector of the Arctic Ocean

**D. A. Iakovleva[a, b, *], I. L. Bashmachnikov[a, b], and D. A. Kuznetsova[a, b]**

[a] *St. Petersburg State University, St. Petersburg, Russia*

[b] *Nansen International Environmental and Remote Sensing Center, St. Petersburg, Russia*

**e-mail: d.iakovleva@spbu.ru*

Received June 9, 2022; revised September 7, 2022; accepted September 12, 2022

**Abstract**—In this study, we investigate the impact of variability of the Atlantic Meridional Overturning Circulation (AMOC) on water temperature of the upper 100-m layer of the North Atlantic and Arctic Ocean. We use three datasets (ARMOR-3D, SODA3.4.2, and ORAS4) with different spatial resolutions and coverage of different time periods. The temperature variability is decomposed into its natural modes using empirical orthogonal functions (EOF). The second EOF, which accounts for 20–27% of variance of water temperature in the upper ocean, is associated with a change in the AMOC intensity. The time variability of the principal component of this mode has a high correlation with the AMOC (0.6–0.9 depending on the dataset and AMOC index used). The AMOC has the highest impact on water temperature in the Irminger and Labrador seas. The related amplitude of water temperature fluctuations reaches 1.5–2°C in the central Irminger Sea, one of the key areas of deep convection. Intensification of the AMOC over most of the North Atlantic and in the Norwegian Sea leads to a decrease in water temperature over most of the Greenland Sea, in the Barents Sea, and north of Spitsbergen.

**Keywords:** Atlantic Meridional Overturning Circulation, water temperature, EOF, North Atlantic, Arctic Ocean

**DOI:** 10.1134/S0001437023020133

## INTRODUCTION

The Atlantic Meridional Overturning Circulation (AMOC) characterizes the generalized transfer of mass (heat, salt) in the meridional direction. Heat advection by the upper branch of the AMOC to the subpolar North Atlantic is redistributed in the Iceland Basin between two main extensions of the North Atlantic Current: the Irminger Current, which transports heat into the Subpolar Gyre (the Irminger and Labrador seas), and the Norwegian Current, which transports heat over the Nordic Seas. A relatively small fraction of the total heat flow also enters the Norwegian Current with an extension of the Irminger Current that skirts Iceland from the west (the North Icelandic Irminger Current).

The lower branch of the AMOC, the AMOC deep return flow, is formed in deep convection zones in the Irminger, Labrador, and Greenland seas, where intense heat loss by the ocean is observed in winter. For a long time, it was believed that the variability of the volume of deep water formed in the Labrador Sea [31] is one of the most significant factors of the AMOC's variability. Variability in the volume of deep waters generated in the Irminger Sea is a much more important source of interannual variability of the AMOC [6, 20]. Until the beginning of the 2000s, the convection intensity was rather low, but by the mid-2010s, deep convection zone in the eastern Subpolar Gyre (in the Irminger Sea and south of Cape Farewell) exceeded the deep convection zone in the Labrador Sea for the first time since the 1950s, while the volume of newly formed Irminger Intermediate Water became comparable to that in the Labrador Water. According to literature sources, this situation persisted at least until the end of the 2010s. [25].

The objective of this study is to identify the contribution of the AMOC to the temperature variability in the upper North Atlantic and Atlantic sector of the Arctic Ocean (AO). It is especially important to evaluate the influence of the AMOC on the temperature of the upper layer of Subpolar Gyre, where the main deep convection zones are formed. The possible influence of AMOC heat fluxes on water temperature in this region can form feedbacks that stabilize the AMOC [19].

The possible influence of the AMOC on the temperature of Atlantic water in the Arctic Ocean follows from the observed nature of the transport of temperature anomalies by the system of surface currents in the North Atlantic. In particular, it has been demonstrated that the temperature variability in the North Atlantic Current in the Faroe–Shetland Strait can penetrate far into the Eurasian Basin of the Arctic Ocean [1, 17, 23]. It is also possible to trace the spread of sea surface temperature anomalies from regions of the tropical North Atlantic to

the Fram Strait (over the course of approximately 4 years) and farther, along the shelf edge of the Eurasian Basin, to the central regions of the Arctic Ocean [9]. It is assumed that such propagation of temperature anomalies in the ocean is supported by large-scale mechanisms of ocean–atmosphere interaction, which in turn cause an increase in atmospheric heat transport to the Arctic. This, in particular, has a significant effect on the interannual variability of the sea ice area in the Arctic [2].

The dynamics of the AMOC in the North Atlantic can be reliably estimated from the start of operation of the RAPID Transatlantic Observations dataset in the first half of the 2000s [30]. From the first half of the 1990s, the AMOC dynamics can be estimated from the results of joint processing of satellite altimetry data and Argo floats, from individual observations of currents for some years, and from indirect indicators [12, 15, 16, 21]. All available evidence points to gradual weakening of the AMOC from the 1960s to the 1980s; in the second half of the 1990s, it experienced a short-term intensification. During this period, the volume, temperature, and salinity of Atlantic water in the Nordic Seas, and, somewhat later, in the Eurasian Basin of the Arctic Ocean, increased and remained high with respect to the climatic average until the mid-1990s [9, 17]. Since the mid-1990s. there is a local decrease in the intensity of the AMOC [15], which was accompanied by a decrease in the heat flow and in the transport of the West Spitsbergen Current [17]. In the mid 2000s, a local AMOC maximum was observed, after which a fairly rapid decrease in the AMOC intensity began, which continued until the 2010s, which was also noted from direct observations on the RAPID transect (26° N) [15, 21]. It was accompanied by a decrease in deep convection in the Labrador and Irminger seas [4] and weakening of the currents of the Subpolar Gyre (the Labrador, East Greenland, West Greenland, and Irminger currents) [5]. Later, the AMOC discharge rate stabilized at lower values. The vast majority of modern climate models predict a long-term trend towards a further deceleration of the AMOC, by an average of 30% by the end of the 21st century [29]. Decadal and intradecadal fluctuations noted earlier are superimposed on this trend.

Of course, the AMOC is only one of the mechanisms that regulate fluctuations in ocean heat flux in the subpolar and polar regions. Based on analysis of in situ and model data, many researchers attribute the increase in the intensity of the northward heat transport over the North European Basin in the 1990s to a regional increase in the atmospheric cyclonic circulation over the basin and a weakening of the heat flux from the sea-surface in this region [2, 17]. The intensity of heat flux in this region is also associated with the influence of large-scale atmospheric structures characterized by the North Atlantic Oscillation (NAO), East Atlantic Oscillation, and Wangerheim–Giers circulation indices [17, 28]. On the other hand, variability of the NAO and AMOC dynamics are presumably related to each other through numerous direct and feedback mechanisms (see, e.g., [2, 26]).

## MATERIALS AND METHODS

We have studied the temperature variability of the upper 100-m layer of the North Atlantic Ocean and Atlantic sector of the Arctic Ocean (45–90° N and 70° W–140° E; Fig. 1a). The analysis was carried out using the mean monthly water temperature data of three datasets: ARMOR-3D[1], SODA3.4.2[2], and ORAS4[3]. ARMOR-3D has better spatial resolution, while ORAS4 and SODA3.4.2 have longer datasets.

ARMOR-3D (1993–2020) is a dataset which merges in situ and satellite data. The dataset is provided on a regular grid with a spatial resolution of 0.25° × 0.25° [18, 22]. The ARMOR-3D dataset integrates in situ temperature profiles of the World Ocean Database (WOD) and other observational databases [18], as well as satellite sea surface temperature (SST) on a regular grid of the Reynolds dataset, and AVISO satellite altimetry data. In order to reproduce 3D water temperature fields, at the first stage, satellite data are interpolated downwards using a multiple linear regression to form "synthetic" vertical temperature profiles. Then, the in situ and synthetic profiles are combined by optimal interpolation into a 3D dataset of monthly water temperature fields [27]. Due to the abovementioned peculiarities of its construction, the ARMOR-3D dataset well reproduces the temperature variability of the upper ocean in tropical and subpolar regions, but poorly reflects the variability of the subsurface water temperature of the ice-covered waters of the Arctic Ocean.

The SODA3 ocean reanalysis (v. 4.2, Simple Ocean Data Assimilation, 1980–2020) has a spatial resolution of 0.5° × 0.5°. The SODA3.4.2 reanalysis is based on the MOM5 ocean dynamics model with the SIS1 ice block. The model assimilates in situ temperature profile data (from WOD), SST data (International Comprehensive Ocean–Atmosphere Dataset, ICOADS observations), and satellite SST data [14]. Atmospheric forcing at the upper boundary of the SODA3.4.2 model is from the ERA-Interim atmospheric reanalysis.

ORAS4 (Ocean ReAnalysis System 4, 1958–2017) is based on the NEMO V3.0 ocean model. It has a spatial resolution of 1° × 1° [10]. Depending on the modeling period, ERA-40 atmospheric reanalysis (from 1957 to 1989), ERA-Interim (from 1989 to 2009), or ECMWF NWP (from 2010) data are used as the atmospheric forcing. ORAS4 assimilates in situ vertical water temperature and salinity profiles, data from moorings and sensors mounted on marine animals, as well as satellite SST and sea ice concentration data.

The fields of spatiotemporal variability of the temperature of the upper ocean were decomposed into characteristic modes of their variability using empirical orthogonal functions (EOF), which makes it possible to identify the characteristic spatial structures of

[1] http://marine.copernicus.eu/
[2] http://www.soda.umd.edu/
[3] https://www.cen.uni-hamburg.de/en/icdc/data/ocean/easy-init-ocean/ecmwf-ocean-reanalysis-system-4-oras4.html

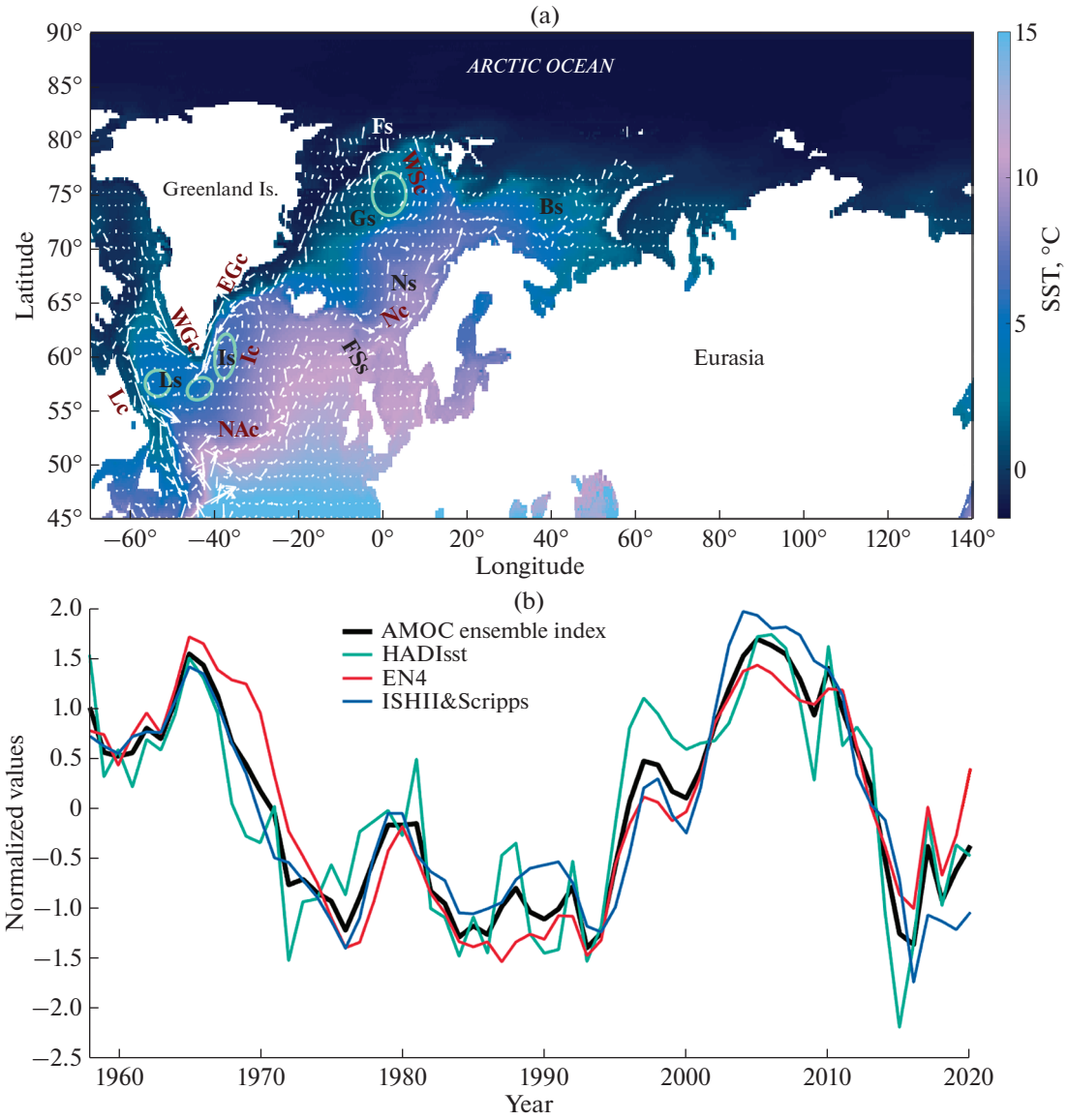


**Fig. 1.** (a) Study area showing average SST field and current velocities for 1993–2020 from the ARMOR-3D dataset. Green ellipses show areas where winter convection is the most frequent and exceeds 1000 m. GC is the Greenland Current; WSC is the West Spitsbergen Current; LC is the Labrador Current; NC is the Norwegian Current; NAC is the North Atlantic Current; IC is the Irminger Current; FS is the Fram Strait; FSS is the Faroe-Shetland Strait; (b) interannual variability of normalized values of three AMOC indices from HADIsst (temperature index), EN4 (salinity index), ISHII&Scripps (salinity index) datasets, and the AMOC ensemble index since 1958.

variation of the parameters with the similar temporal variability, as well as to determine the contribution of each of these structures to the total variance of the initial temperature variability of the selected region [7]. The modes obtained with EOF are orthogonal to each other; i.e., it can be anticipated that the physical processes describing different EOF modes are different, although this is not always the case. An additional difficulty in interpreting the EOF results is that various processes that form the observed variability of water temperature are often interrelated.

The intensity of the AMOC over the entire observation period (Fig. 1b) was characterized by both temperature and salinity indices [15]. According to this study cited above, the salinity indices were determined as the average salinity of the North Atlantic between 45–65° N in the 0–1500 m layer. One index was calculated using the merged in situ databases ISHII[4] (1946–2015) and Scripps[5] (2004–2020), while the other, using the EN4 database[6] (1946–2020). The temperature index HADIsst (1871–2020), also obtained from EN4 data, represents the difference

[4] http://rda.ucar.edu/datasets/ds285.3/
[5] http://www.argo.ucsd.edu/Gridded_fields.html
[6] https://www.metoffice.gov.uk/hadobs/en4/

**Table 1.** Variance (%) of the first three EOFs of water temperature in 0–100 m layer from ARMOR-3D, SODA3.4.2, and ORAS4 datasets

| | EOF 1 | EOF 2 | EOF 3 |
|---|---|---|---|
| ARMOR-3D | 41 | 27 | 9 |
| SODA3.4.2 | 43 | 21 | 8 |
| ORAS4 | 41 | 20 | 10 |

between the SST in the Subpolar Gyre and the global mean SST [13]. All these indices well reproduce the variability of the AMOC obtained both from analysis of RAPID observations since 2004 and from the results of joint analysis of altimetry data and Argo float trajectories since the early 1990s. [15]. The AMOC ensemble index is formed as the mean between the three above-mentioned indices, prior to their normalization.

## RESULTS AND DISCUSSION

According to the results of the EOF analysis of water temperature in the North Atlantic and Arctic Ocean, the variances of the first three EOFs of water temperature in total exceed 70% for any of the 3 datasets used (Table 1).

The first EOF characterizes the general tendency of the temperature of the upper ocean to increase over the entire period of observations (Appendix 1). This mode characterizes the warming of the upper ocean and, according to all three databases, makes the largest contribution to the total variance, exceeding 40% (Table 1).

The variance of the second EOF is also quite large, 27% for ARMOR-3D, 21% for SODA3.4.2, and 20% for ORAS4 (Table 1). The second EOF of water temperature is of greatest interest to us, since its principal component (PC) has high (from 0.60 to 0.90) correlations with all AMOC indices, including the ensemble index (Table 2; Fig. 2). This mode mainly determines the interdecadal variability in the temperature of the upper ocean. The associated water temperature variability reflects a downward trend in AMOC intensity from the mid-1960s to the mid-1970s, a further increase from the 1990s to the mid-2000s, a new weakening until the early 2010s, and a weakly expressed intensification of the AMOC in the late 2010s. The weakening and subsequent intensification of the AMOC at the beginning of the 21st century agrees with its direct observations since 2004 [30], while weakening of the AMOC in the 1960s–1970s is confirmed by an analysis of the state of coral reefs and direct hydrographic observations for individual years [24].

The third EOF describes about 10% of the total water temperature variance (Table 1; Appendix 2), characterizing a shorter-term intradecadal variability of water temperature.

The relationship between the variability of the second PC and AMOC variability makes it possible to reveal the influence of the AMOC on the spatial structure of the temperature of the upper layer of the ocean (Fig. 3). The spatial distributions of temperature anomalies associated with the AMOC dynamics are similar for all three datasets. In the subpolar North Atlantic and in the Nordic Seas, as the intensity of the AMOC increases, the temperature of the upper 100-m layer of the ocean rises (Fig. 3). The strongest increase in water temperature is observed in the central Irminger Sea, northeastern Labrador Sea, and along the Labrador Current. The southern and southeastern parts of the Norwegian Sea are also warming. However, in the Greenland and Barents seas, as well as an area north of Svalbard, the SODA3.4.2 and ORAS4 reanalyses show a decrease in the temperature of the upper 100-m layer with increasing AMOC intensity. In ARMOR-3D, against a general increase in water temperature in a significant part of the Nordic Seas, there is also a slight decrease in water temperature north of Svalbard and in the eastern Barents Sea. In the upper Kara, Laptev, and East Siberian seas, where the influence of Atlantic water advection is weak, no relationship between the upper ocean temperature and AMOC variability can be traced.

Differences in the characteristics of the colling regions with intensification of the AMOC in the ARMOR-3D dataset may be associated with different lengths of the time series. Thus, EOF2 of the relatively short ARMOR-3D series includes part of the current warming trend, which can be seen from a certain slope of the second ARMOR-3D PC with respect to the corresponding PCs in SODA3.4.2 and ORAS4 for 1993–2020 (Fig. 2). The virtually nonexistent variability of the second EOF in the ARMOR-3D dataset at high latitudes of the Arctic Basin, in contrast to the

**Table 2.** Correlations of the second PC of water temperature in 0–100 m layer with AMOC indices. Significance level of correlations for each dataset is indicated in brackets in first column of table

| Dataset/AMOC index | AMOC HADIsst | AMOC ISHII&Scripps | AMOC EN4 | Ensemble index AMOC |
|---|---|---|---|---|
| ARMOR-3D, PC2 (0.38) | 0.79 | 0.77 | 0.88 | 0.86 |
| SODA3.4.2, PC2 (0.31) | 0.80 | 0.66 | 0.61 | 0.73 |
| ORAS4, PC2 (0.25) | 0.92 | 0.85 | 0.80 | 0.90 |

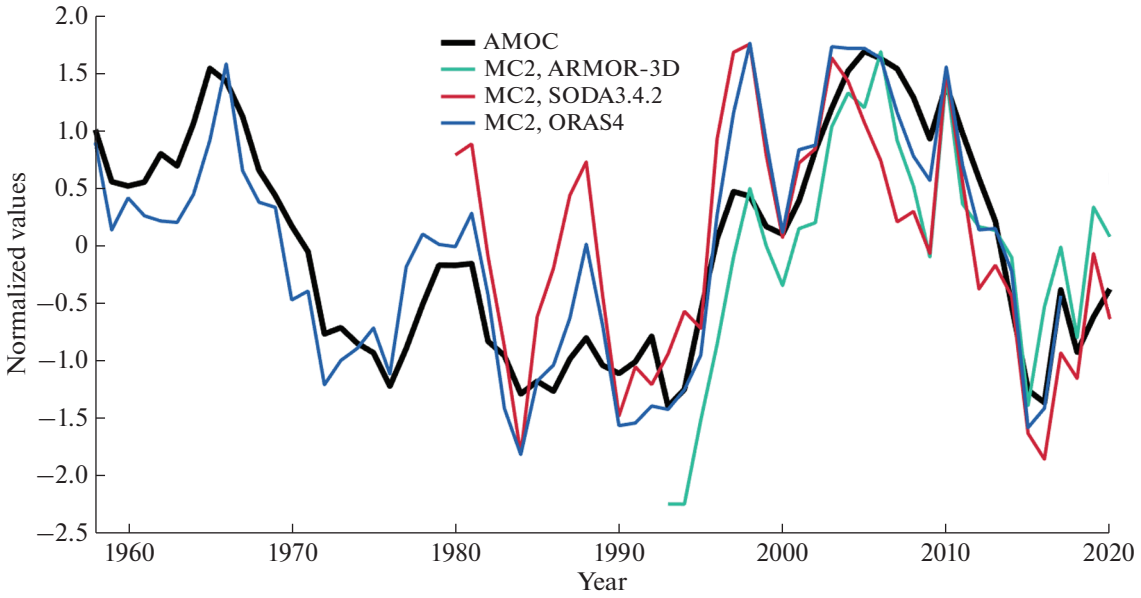


**Fig. 2.** Interannual variability of the AMOC ensemble index (black line) and the principal components of the EOF decomposition of water temperature from ARMOR-3D (second mode, since 1993), SODA3.4.2 (second mode, since 1980), and ORAS4 (second mode, since 1958). Spatial distibutions of the corresponding EOF are shown in Fig. 3.

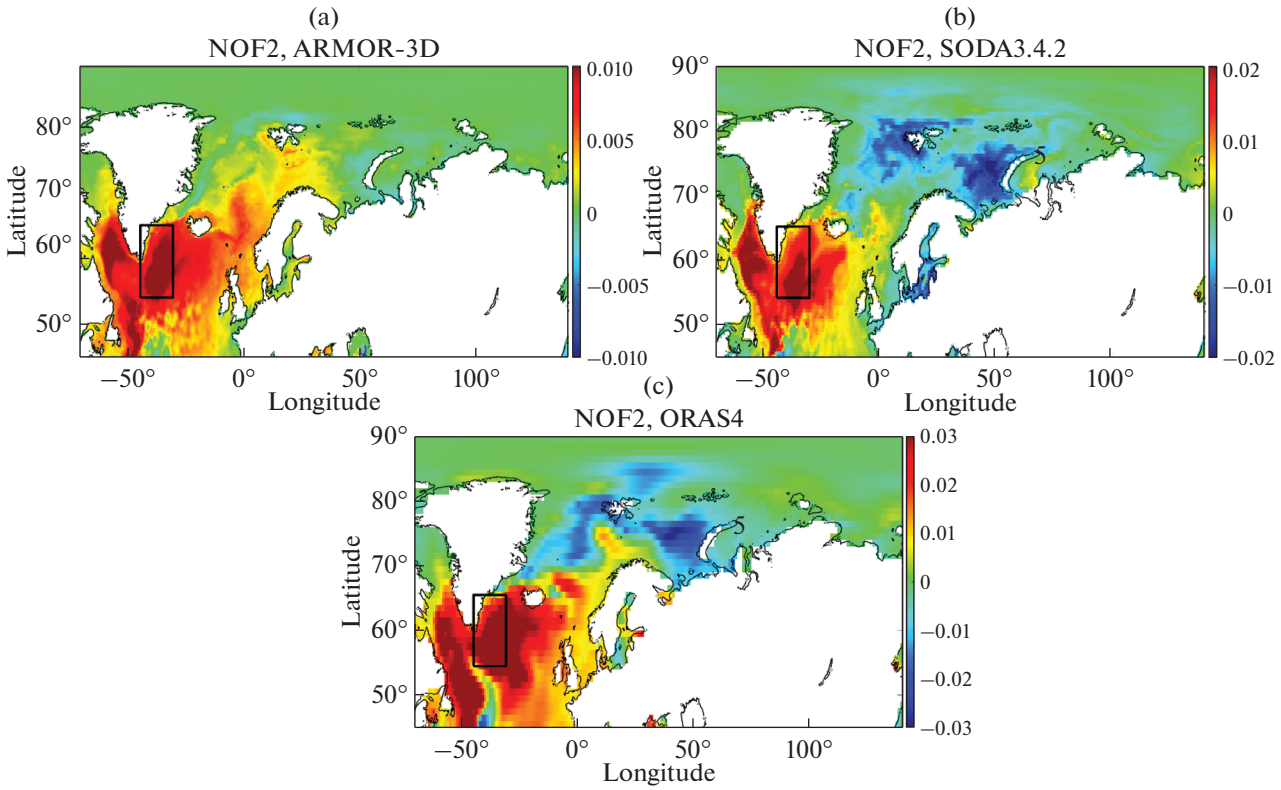


**Fig. 3.** Spatial distributions of amplitude of the second EOF of water temperature in 0–100-m layer, associated with the AMOC variability: (a) ARMOR-3D data, (b) SODA3.4.2 data, (c) ORAS4 data. Area of the Irminger Sea is delimited by the black rectangle.

SODA3.4.2 and ORAS4 reanalyses, is due to the fact that the ARMOR-3D data are based exclusively on satellite and observational data, which are extremely scarce in the ice-covered regions. This does not allow reliably revealing the spatiotemporal variability of water characteristics in these areas of the Arctic Ocean.

The amplitude of water temperature fluctuations in the 0–100 m layer as a result of changes in the AMOC intensity in the deep convection zone (see [3, 8]) in the central Irminger Sea is maximum, 1.5–2°C. This result was confirmed by additional EOF analysis covering only the Irminger Sea (black box in Fig. 3). In this limited region, the AMOC variability govern 61% in ORAS4, 78% in SODA3.4.2, and 85% in ARMOR-3D of water temperature dispersion in the upper 100-m ocean. The correlation of the AMOC ensemble index with the corresponding PCs of any of the three datasets was 0.9.

## CONCLUSIONS

Based on analysis of several datasets with different lengths of the time series, it was shown that the AMOC forms the second EOF of the upper ocean temperature of the North Atlantic and Atlantic sector of the Arctic Ocean. The contribution of this EOF is 20–27% of the total variance of the water temperature. In particular, we have shown that the AMOC makes a significant contribution to the decrease in temperature of the upper ocean from the mid-1960s to the mid-1970s, the increase from the 1990s to the mid-2000s, and a new decline from the mid-2000s to the mid-2010s, which was previously noted for different areas of the Atlantic and in the southeastern part of the Nordic Seas (see, e.g., [9, 11, 12]).

Our results show that the effect of the AMOC is the largest for the upper central Irminger Sea, where the variability of the AMOC intensity, observed during recent decades, leads to an amplitude of temperature fluctuations of 1.5–2°C in the upper 100-m layer. This can significantly affect the convection intensity in this key region.

The SODA3.4.2 and ORAS4 data also show that an increase in the AMOC intensity leads to a decrease in temperature over most of the Barents Sea (primarily in its eastern part), in the Greenland Sea, and north of Svalbard. Observations show that the long-term 80-year variability in the temperature of the Atlantic water in the Arctic is in phase with the variability in the temperature of the upper layer of the North Atlantic, however the shorter-term variability might be out-of-phase [23]. Note also that, in this paper, we are talking not so much about the Atlantic waters, but about the upper 100-m layer of the sea. The mechanisms of the decrease in temperature of the upper ocean in the northern areas of the Nordic Seas and adjacent part of the Arctic Ocean with an increase in the AMOC intensity require further investigation.

*APPENDIX 1*

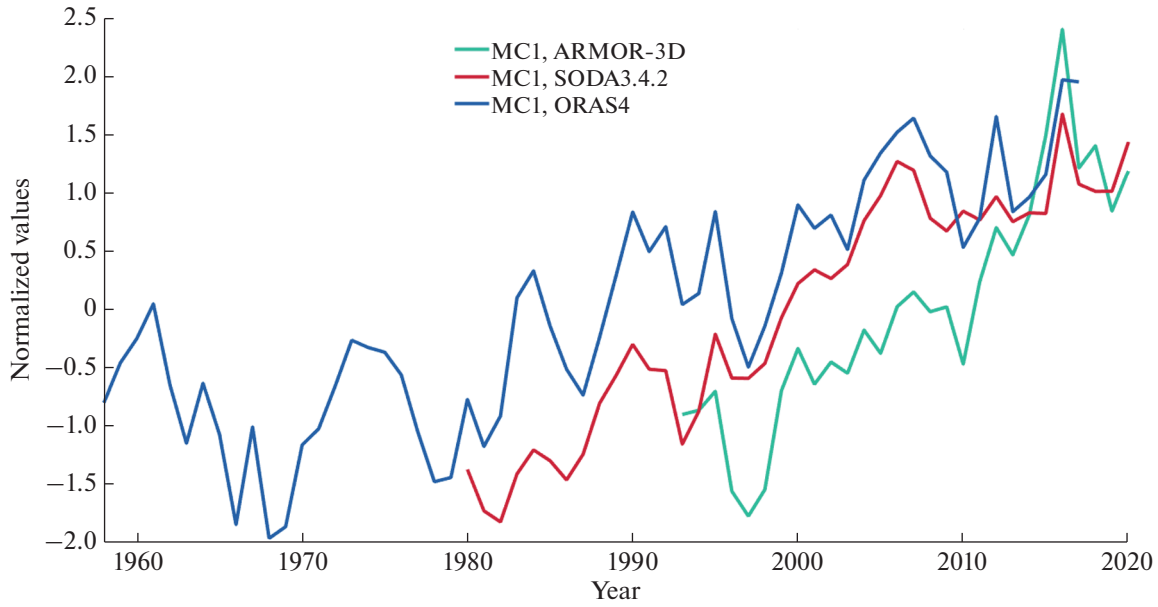


**Fig. A1.** Interannual variability of the EOF principal components from the ARMOR-3D (first mode, since 1993), SODA3.4.2 (first mode, since 1980), and ORAS4 (first mode, since 1958) datasets.

*APPENDIX 2*

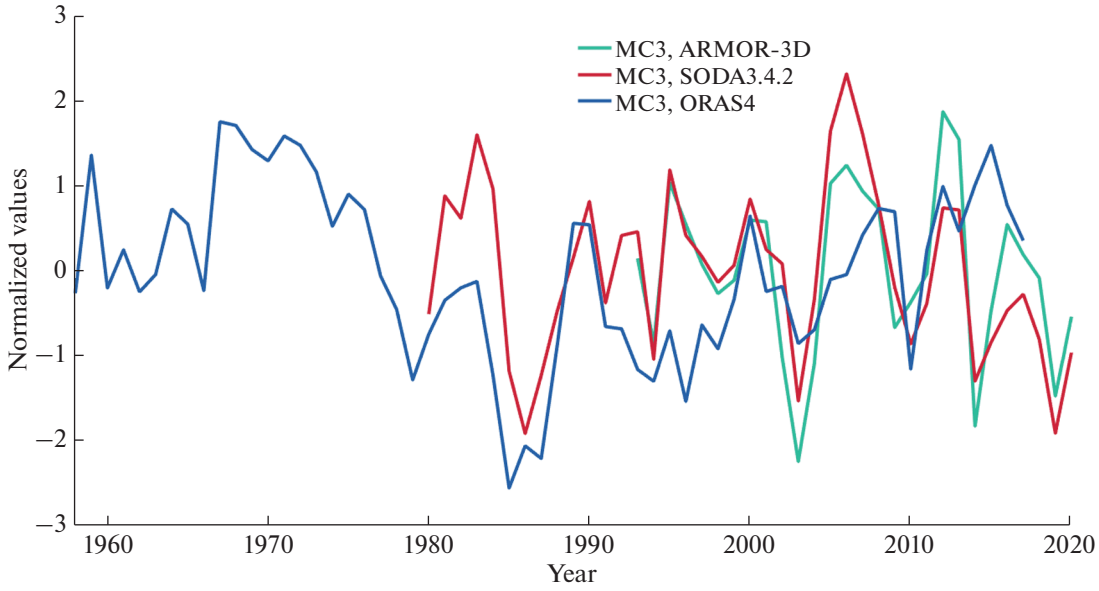


**Fig. A2.** Interannual variability of the EOF principal components from the ARMOR-3D (third mode, since 1993), SODA3.4.2 (third mode, since 1980), and ORAS4 (third mode, since 1958) datasets.

## FUNDING

The study was supported by the Ministry of Science and Higher Education of the Russian Federation (project no. 13.2251.21.0006, identifier RF-225121X0006, agreement no. 075-10-2021-104 in the Russian Federation "Electronic Budget" information system).

## REFERENCES

1. G. V. Alekseev, A. E. Vyazilova, N. I. Glok, et al., "The effect of water temperature anomalies at low latitudes of the ocean on Arctic climate variations and their predictability," Arktika: Ekol. Ekon. **3** (35), 73–83 (2019). https://doi.org/10.25283/2223-4594-2019-3-73-83
2. G. V. Alekseev, S. I. Kuzmina, N. I. Glok, et al., "Influence of Atlantic on the warming and reduction of sea ice in the Arctic," Led Sneg. **57** (3), 381–390 (2017). https://doi.org/10.15356/2076-6734-2017-3-381-390
3. I. L. Bashmachnikov, A. M. Fedorov, A. V. Vesman, et al., "Thermohaline convection in the subpolar seas of the North Atlantic and the North European basin of the Arctic Ocean according to satellite and field data. Part 1: Localization of convection regions," Sovrem. Probl. Distantsionnogo Zondirovaniya Zemli Kosmosa **15** (7), 184–194 (2018). https://doi.org/10.21046/2070-7401-2018-15-7-184-194
4. I. L. Bashmachnikov, A. M. Fedorov, A. V. Vesman, et al., "Thermohaline convection in the subpolar seas of the North Atlantic and the North European basin of the Arctic Ocean according to satellite and field data. Part 2: Convection intensity indices," Sovrem. Probl. Distantsionnogo Zondirovaniya Zemli Kosmosa **16** (1), 191–201 (2019). https://doi.org/10.21046/2070-7401-2019-16-1-191-201
5. T. V. Belonenko, A. M. Fedorov, I. L. Bashmachnikov, and V. R. Fuks, "Current intensity trends in the Labrador and Irminger seas from satellite altimetry data," Issled. Zemli Kosmosa, No. 2, 3–12 (2018). https://doi.org/10.7868/S020596141802001X
6. D. A. Kuznetsova and I. L. Bashmachnikov, "On the mechanisms of variability of the Atlantic Meridional Overturning Circulation (AMOC)," Oceanology **61** (6), 803-814 (2021). https://doi.org/10.1134/S0001437021060072
7. A. N. Lyakhov, "Modern methods of data processing in geophysics," in *Proceedings of the International Baikal Youth Scientific School on Fundamental Physics and the Conference of Young Scientists "Physical Processes in Space and Near-Earth Environment"* (ISZF SO RAN, Irkutsk, 2006), pp. 39–46.
8. A. M. Fedorov, I. L. Bashmachnikov, T. V. "Belonenko, Localization of deep convection areas in the seas of the North European Basin, Labrador and Irminger," Vestn. S.-Peterb. Univ. Nauki Zemle **63** (3), 345–362 (2018). https://doi.org/10.21638/spbu07.2018.306
9. G. V. Alekseev, A. V. Smirnov, A. V. Pnyushkov, et al., "Changes of fresh water content in the upper layer of the Arctic Basin in the 1950s–2010s," Fundam. Prikl. Gidrofz. **14** (4), 25–38 (2021). https://doi.org/10.7868/S2073667321040031
10. M. A. Balmaseda, K. Mogensen, and A. T. Weaver, "Evaluation of the ECMWF ocean reanalysis system

ORAS4," Q. J. R. Meteorol. Soc. **139** (674), 1132–1161 (2013).
https://doi.org/10.1002/qj.2063

11. H. L. Bryden, W. E. Johns, B. A. King, et al., "Reduction in ocean heat transport at 26 N since 2008 cools the eastern subpolar gyre of the North Atlantic Ocean," J. Clim. **33** (5), 1677–1689 (2020).
https://doi.org/10.1175/JCLI-D-19-0323.1
12. L. Caesar, G. D. McCarthy, D. J. R. Thornalley, et al., "Current Atlantic meridional overturning circulation weakest in last millennium," Nat. Geosci. **14** (3), 118–120 (2021).
https://doi.org/10.1038/s41561-021-00699-z
13. L. Caesar, S. Rahmstorf, A. Robinson, et al., "Observed fingerprint of a weakening Atlantic Ocean overturning circulation," Nature **556** (7700), 191–196 (2018).
https://doi.org/10.1038/s41586-018-0006-5
14. J. A. Carton, G. A. Chepurin, and L. Chen, "SODA3: A new ocean climate reanalysis," J. Clim. **31** (17), 6967–6983 (2018).
https://doi.org/10.1175/JCLI-D-18-0149.1
15. X. Chen and K. K. Tung, "Global surface warming enhanced by weak Atlantic overturning circulation," Nature **559** (7714), 387–391 (2018).
https://doi.org/10.1038/s41586-018-0320-y
16. E. Frajka-Williams, I. J. Ansorge, J. Baehr, et al., "Atlantic meridional overturning circulation: Observed transport and variability," Front. Mar. Sci. **6** (260) (2019).
https://doi.org/10.3389/fmars.2019.00260
17. M. J. Karcher, R. Gerdes, F. Kauker, and C. Köberle, "Arctic warming: Evolution and spreading of the 1990s warm event in the Nordic seas and the Arctic Ocean," J. Geophys. Res.: Oceans **108** (C2) (2003).
https://doi.org/10.1029/2001JC001265
18. G. Larnicol, S. Guinehut, M. H. Rio, et al., "The global observed ocean products of the French Mercator project," in *Proceedings of the Symposium on 15 Years of Progress in Radar Altimetry,* European Space Agency Special Publication SP-614 (2006).
19. A. Levermann and A. Born, "Bistability of the Atlantic subpolar gyre in a coarse-resolution climate model," Geophys. Res. Lett. **34** (24) (2007).
https://doi.org/10.1029/2007GL031732
20. M. S. Lozier, F. Li, S. Bacon, et al., "A sea change in our view of overturning in the subpolar North Atlantic," Science **363** (6426), 516–521 (2019).
21. G. D. McCarthy, P. J. Brown, C. N. Flagg, et al., "Sustainable observations of the AMOC: Methodology and technology," Rev. Geophys. **58** (1) (2020).
22. B. B. Nardelli, S. Guinehut, A. Pascual, et al., "Towards high resolution mapping of 3-D mesoscale dynamics from observations," Ocean Sci. **8** (5), 885–901 (2012).
https://doi.org/10.5194/os-8-885-2012
23. I. Polyakov and M. Johnson, "Arctic decadal and interdecadal variability," Geophys. Res. Lett. **27** (24), 4097–4100 (2000).
https://doi.org/10.1029/2000GL011909
24. S. Rahmstorf, J. E. Box, G. Feulner, et al., "Exceptional twentieth-century slowdown in Atlantic Ocean overturning circulation," Nat. Clim. Change **5** (5), 475–480 (2015).
https://doi.org/10.1038/nclimate2554
25. S. Rühs, E. C. Oliver, A. Biastoch, et al., "Changing spatial patterns of deep convection in the subpolar North Atlantic," J. Geophys. Res.: Oceans **126** (7), e2021JC017245 (2021).
https://doi.org/10.1029/2021JC017245
26. K. Våge, R. S. Pickart, A. Sarafanov, et al., "The Irminger gyre: Circulation, convection, and interannual variability," Deep-Sea Res. I **58** (5), 590–614 (2011).
https://doi.org/10.1016/j.dsr.2011.03.001
27. N. Verbrugge, S. Mulet, and S. Guinehut, "Quality information document For global ocean observation-based products GLOBAL_ANALYSIS_PHYS_001_020," Copernicus, EU (2017). https://resources.marine.copernicus.eu/documents/QUID/CMEMS-GLOQUID-001-021.pdf.
28. A. V. Vesman, I. L. Bashmachnikov, P. A. Golubkin, and R. P. Raj, "The coherence of the oceanic heat transport through the Nordic seas: Oceanic heat budget and interannual variability," Ocean Sci. Discuss., 1–24 (2020).
https://doi.org/10.5194/os-2020-109
29. M. Visbeck, "Power of pull," Nature **447** (7143), 383–383 (2007).
https://doi.org/10.1038/447383a
30. D. L. Volkov, C. S. Meinen, C. Schmid, et al., "Atlantic meridional overturning circulation and associated heat transport," in *State of the Climate in 2019,* Ed. by J. Blunden and D. S. Arndt (American Meteorological Society, 2020), pp. 159–163.
https://doi.org/10.1175/BAMS-D-20-0105.1
31. I. Yashayaev, "Hydrographic changes in the Labrador Sea, 1960–2005," Prog. Oceanogr. **73** (3–4), 242–276 (2007).
https://doi.org/10.1016/j.pocean.2007.04.015

SPELL: 1. distibutions